



HAL
open science

Superinsulating composite aerogels from polymethylsilsesquioxane and kapok fibers

Aravind Parakkulam Ramaswamy, Arnaud Rigacci

► **To cite this version:**

Aravind Parakkulam Ramaswamy, Arnaud Rigacci. Superinsulating composite aerogels from polymethylsilsesquioxane and kapok fibers. *Materials Chemistry and Physics*, 2021, 261, pp.124252. 10.1016/j.matchemphys.2021.124252 . hal-03511785

HAL Id: hal-03511785

<https://minesparis-psl.hal.science/hal-03511785>

Submitted on 3 Feb 2023

HAL is a multi-disciplinary open access archive for the deposit and dissemination of scientific research documents, whether they are published or not. The documents may come from teaching and research institutions in France or abroad, or from public or private research centers.

L'archive ouverte pluridisciplinaire **HAL**, est destinée au dépôt et à la diffusion de documents scientifiques de niveau recherche, publiés ou non, émanant des établissements d'enseignement et de recherche français ou étrangers, des laboratoires publics ou privés.



Distributed under a Creative Commons Attribution - NonCommercial 4.0 International License

Superinsulating composite aerogels from polymethylsilsesquioxane and kapok fibers

Aravind Parakkulam Ramaswamy ^{*a}, Arnaud Rigacci ^{**a}

MINES ParisTech, PSL Research University, PERSEE, Centre procédés, énergies renouvelables et systèmes énergétiques, rue Claude Daunesse, CS 10207, 06904, Sophia Antipolis, France.

*Email - * aravind.parakkulam_ramaswamy@mines-paristech.fr; aravind.niist@gmail.com;*

*** arnaud.rigacci@mines-paristech.fr*

Abstract

A facile method to synthesize light weight thermally superinsulating composite aerogel is being presented here. A polymethylsilsesquioxane (PMSQ) – cellulose composite aerogel starting from a trifunctional precursor viz. methyltrimethoxysilane (MTMS) and kapok fibers have been synthesized. Kapok fibers have been employed as they have a homogeneous hollow structure and also possess intrinsic low density. A PMSQ-Kapok composite aerogel with a density as low as 0.053 gcm^{-3} with a thermal conductivity of $0.018 \text{ W.m}^{-1}.\text{K}^{-1}$ in room conditions has been synthesized. Besides, a flexural strength (at maximum stress) of $108 \text{ kPa} \pm 21$ has been obtained through three points bending test. All the composite aerogels are mesoporous as characterized by N_2 sorption isotherms and hydrophobic as shown by sessile drop experiments. On comparison with the earlier reported works and with some of the commercially available aerogel composites, the current results seem promising. For demonstrating the real application purpose, thin composite aerogel sheets have also been synthesized which could be easily rolled/bended.

Keywords: Materials for energy; Composites; aerogels; Natural fibers; Thermal properties; Mechanical properties

Introduction

Aerogels are low density and predominantly mesoporous materials consisting of a three-dimensional network. They possess excellent properties due to their low density, high surface area and their peculiar internal nanostructure [1,2]. Silica aerogels have drawn most of the interest after their discovery by Kistler some eight decades ago [3]. However, the mechanical fragility of silica aerogels along with their cost of production (including raw materials) remains a major drawback and this has clearly prevented its widespread application to a greater extend.

For improving the mechanical properties of silica aerogels, two common procedures/methods are reported well in the literatures: 1) by crosslinking with reactive molecules [4-9] and 2) by employing a macroscopic fibrous “template” where both inorganic and organic fibers are utilized [10]. The organic fibers reported include polyester fibers [11], non-woven polypropylene fibers [12], polyamide fibers [13] electro spun polyurethane fibers [14], polyvinylidene fluoride (PVDF) electro spun nanofibers [15], Aramid fibers (KEVLAR®) [16], nanofibrillated cellulose [17], Pectin nanofibers [18] as well as Lyocell fibers [19,20]. The reported inorganic fiber template includes ceramic fibers [21], glass fibers [22], sepiolite fibers [23], silica fibers [24], attapulgite fibers [25], zirconia fibers [26] and aluminium borate whiskers [27]. A less common route (method 3) to improve the mechanical properties is by impregnation or by the dispersion of micro/nano secondary phase such as polymers [28], nanoparticles [29], ceramics [30] etc.

The crosslinking (method 1 here-above) leads to the mechanical improvement of the aerogel. However, as a side effect, there is an increase of density, decrease in the specific porosity and specific surface area (SSA) [10]. Most importantly for some strategic applications, the thermal conductivity of such crosslinked aerogels is generally in the range of 0.040-0.130 W.m⁻¹.K⁻¹ which is extremely high regarding thermal insulation objectives [5, 8, 10]. The dispersion/insertion of fibers (method 2) prevents the shrinkage during synthesis and improve the mechanical properties of aerogels [10]. However, here also the real challenge is to preserve the insulation properties and high SSA [10].

Natural fibers are environmentally friendly and composite aerogels employing these templates have been reported by many researchers [10]. Amongst others, the use of natural fibers is advantageous as they reduce the carbon footprint of the industrial product [10,18]. As reported below, among natural fibers, cellulose fibers have been employed by many researchers for the reinforcement of silica aerogels as cellulose is easily available and less expensive.

S. Motahari et al. reported a composite made of silica and non-woven cotton mat which was later tested as a sound absorber [31]. E. Rezaei et al prepared cotton composite aerogels with varying silica aerogel (from 20 to 80 wt%) [32]. For the 20 wt% silica aerogel incorporated composite, the density was measured to be 0.078 g.cm⁻³ with a thermal conductivity of 0.025 W.m⁻¹.K⁻¹ and for the 80 wt% silica aerogel incorporated composite, the density was 0.125 g.cm⁻³ with a thermal conductivity of 0.0171 W.m⁻¹.K⁻¹. Short cellulose fiber (Tencel®)-silica composite aerogels were prepared by dispersing cellulose fibers in

polyethoxydisiloxane (PEDS)-based sol [19]. The densities of the composite aerogels ranged from 0.105 g.cm⁻³ to 0.125 g.cm⁻³ and the thermal conductivity (λ) varied from 0.016-0.025 W.m⁻¹.K⁻¹. J. Jaxel et al. studied the influence of fiber length and their volume concentration on the composite aerogel density, thermal conductivity and mechanical properties via 3-point bending test [20]. The composite aerogels were dried both by ambient and supercritical methods and the densities varied from 0.103 g.cm⁻³ to 0.125 g.cm⁻³ and the thermal conductivity (λ) varied from 0.0158-0.0181 W.m⁻¹.K⁻¹. A maximum flexural strength of 184 kPa with a flexural modulus of 6.86 MPa was reported when characterised by 3-point bending tests. A flexural strength of 0.046 MPa with a flexural modulus of 2.59 MPa was also reported by these authors for neat silica aerogel ($\rho = 0.103$ g.cm⁻³ and $\lambda = 0.014$ W.m⁻¹.K⁻¹).

A. Demilecamps et al, impregnated (i.e. method 3) coagulated cellulose wet gels synthesised with PEDS-based solution where the impregnation was performed either by molecular diffusion or by forced flow process [28]. The so-obtained composite had a bulk density between 0.115 and 0.225 g.cm⁻³ and the thermal conductivity varied around 0.027 W.m⁻¹.K⁻¹. Uniaxial compression test was performed on the composite aerogel obtained by the diffusion process and a fractural stress of 6300 kPa with a Youngs modulus of 11.5 MPa was reported. A fractural stress of 1900 kPa with a Young's modulus of 0.07 MPa was measured for neat PEDS derived silica aerogels ($\rho = 0.130$ g.cm⁻³ and $\lambda = 0.015$ W.m⁻¹.K⁻¹). J. Cai et al prepared cellulose-silica composites by employing cellulose hydrogels and tetraethoxysilane (TEOS) [33]. TEOS precursor was hydrolysed in presence of ammonia which was later deposited onto the cellulose network. The density of the composites varied between 0.14 and 0.6 g.cm⁻³ and the thermal conductivity between 0.025 and 0.045 W.m⁻¹.K⁻¹. The tensile and compression tests were performed on the sample with 39 % (w/w) silica ($\rho = 0.34$ g.cm⁻³ and $\lambda = 0.030$ W/m.K) and a tensile and compression strength of 10800 kPa and 1800 kPa respectively were reported. The tensile and compression modulus reported were 48.2 MPa and 7.9 MPa resp. A PEDS derived silica network inside a silylated nanofibrillated cellulose scaffold (NFCS-Si) with superinsulating properties was reported by S. Zhao et al [34]. Thermal conductivity of the composites varied from 0.0138 to 0.0201 W.m⁻¹.K⁻¹ and the densities from 0.122 to 0.146 g.cm⁻³. The best result was obtained where a thermal conductivity of 0.0138 W.m⁻¹.K⁻¹ was reported for a composite of density 0.130 g.cm⁻³. The same composite aerogel had a compressive strength of 300 kPa with an elastic modulus of 2.25 MPa when characterised by uniaxial compression tests. In this study, the PEDS derived neat silica aerogel possessed a compressive strength of 0.3 kPa with an elastic modulus of 1.9

MPa ($\rho = 0.133 \text{ g.cm}^{-3}$ and $\lambda = 0.0125 \text{ W.m}^{-1}.\text{K}^{-1}$). Superflexible composite aerogels are also reported in which bacterial cellulose aerogel phase is incorporated into PMSQ domains [35]. A very low density composite aerogel with a density of 0.09 g.cm^{-3} and a thermal conductivity of $0.015 \text{ W.m}^{-1}.\text{K}^{-1}$ was synthesised. Tensile and compression tests were performed and the composite aerogels prepared had a tensile strength between 1500 – 2200 kPa and the elastic modulus was between 7.5 – 18.6 MPa. Pure PMSQ aerogel was reported to have a tensile strength of around 50 kPa ($\rho = 0.17 \text{ g.cm}^{-3}$). Recently a facile method for the synthesis of composite aerogels was employed by freeze drying the cellulose nanofibril (CNF)/ methyltrimethoxysilane (MTMS)/ fumed silica (FS) suspension [36]. The composite aerogel density varied between 0.005 to 0.03 g.cm^{-3} . However, it has to be noted that the lowest reported thermal conductivity was $0.027 \text{ W.m}^{-1}.\text{K}$ corresponding to a density of 0.016 g.cm^{-3} .

As seen from the previous reported works, it remains very difficult to combine very low density (viz. $< 0.05 \text{ g.cm}^{-3}$) and superinsulating properties along with reasonable mechanical properties (reasonable here stands for a value significantly better than that for pure/neat silica aerogel). In the present work, composite aerogels are synthesised starting with a trifunctional precursor methyltrimethoxysilane (MTMS) and Kapok fibers.

It is important here to mention some of the previous reports of low-density aerogels derived from MTMS precursor alone. In a pioneering work, Starting from MTMS, Kanamori et al. reported transparent monolithic methylsilsesquioxane derived aerogels where the some of the aerogels demonstrated reversible deformation [37]. The density of the aerogels ranges from 0.15 to 0.24 g.cm^{-3} . In another interesting work from the same group, polymethylsilsesquioxane aerogels were synthesised for possible application as thermal super insulators [38]. A very low bulk density of 0.04 g.cm^{-3} with a thermal conductivity of $0.0224 \text{ W.m}^{-1}.\text{K}$ was reported by the authors. In a recent work, Y. Li et al. reported MTMS based aerogels possessing an extremely low density of 0.038 g. cm^{-3} [39]. However, their thermal conductivity reported is 0.0259 W/mK which is relatively high when addressing thermal superinsulation field. In another work from the same group, starting from a trifunctional monomer viz. MTMS, a very low-density aerogel was obtained (0.048 g. cm^{-3}) [40]. However, their thermal conductivity reported is 0.0243 W/mK which is again also relatively too high to tackle superinsulation application.

Kapok fibers are obtained from the seeds of kapok trees (*ceiba pentandra*). Kapok trees are found in Caribbean, central and north Americas, west Africa and south east Asia

[41]. Conventionally the fibers are used for stuffing pillows, bedding, and soft toys. Moreover, due to their excellent buoyancy, kapok fibers are also used as buoyant material (life preservers) and insulation materials against sound and heat [41]. The fibers are soft, silky and have homogeneous hollow tube shape. Their void content is reported to be as high as 80-90% and have a very low density of 0.29 g.cm^{-3} [42]. The hollow nature of the fiber coupled with its low density, makes it an interesting candidate to synthesize very low density and super thermal insulating composite aerogels combined with reasonably good mechanical properties. The aforementioned properties of composite aerogels could thus be very interesting for instance, for space applications where embedded density is of utmost importance. Supercritical (SC) CO_2 drying route was used to obtain monolithic aerogels and the related materials were characterized for bulk and skeletal densities, specific surface area and pore size distributions as well as effective thermal conductivity and morphology (as observed by scanning electron microscopy). The mechanical properties were tested using 3-points bending method. The hydrophobic character was demonstrated via sessile drop tests.

Experimental

Materials

Methyltrimethoxysilane (MTMS), 98% purity, and Hexadecyltrimethylammonium bromide (CTAB), 98% purity were purchased from Sigma-Aldrich. Urea, > 95% purity, Isopropanol, Analytical Reagent, and Glacial acetic acid (HOAc), Analytical Reagent were purchased from Fischer Scientific. Distill water was used to prepare solutions. Kapok fibers were purchased online from the web site artapisserie.fr. Their diameter is around $9 \mu\text{m}$.

Synthesis of Composite aerogels

Different composite aerogels were prepared so as to vary the PMSQ phase weight content (W_{PMSQ}) in the final composite aerogel. Hence, the weight ratio of MTMS/HOAc was varied and ratios of 0.096 0.12 and 0.16, was employed. The weight ratio of 5 mM HOAc solution to urea was maintained at 3.3 for all compositions and the MTMS to surfactant weight ratio was kept constant at 8 too. The fiber concentration with respect to the sol was maintained at 2 wt% for all compositions.

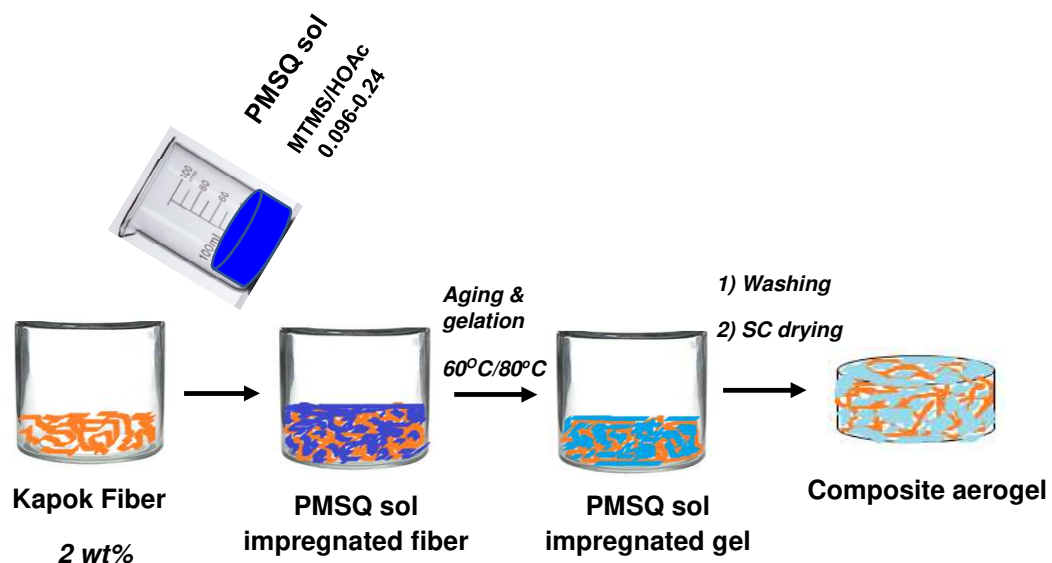
In a typical synthesis for the preparation of 60CA-0.096 (where 60 is the processing temperature ($^{\circ}\text{C}$), CA denotes composite aerogel and 0.096 represents the weight ratio of

MTMS to HOAc) 15 g of urea and 0.6 g of CTAB were stirred well in 50 g of 5 mM HOAc solution for 2-3 minutes at room temperature until a homogeneous solution is formed. To this solution, added 4.8 g of MTMS and the solution was stirred well for 45 minutes. After 45 minutes, 25 g of the sol was weighted out and poured to 0.5 g of Kapok fibers placed in a mold. After pouring the sol, the system (composed of silica-based sol and kapok fibers) is gently tapped with a flat surface so that the fibers are uniformly distributed and to make the system free of any air pockets. The mold was later placed in an oven, which was maintained at 60 °C where the thermal-activated (poly) condensation process leads to the gelation of the particulate sol. After the gelation, some isopropanol was added on top of the composite gel to avoid cracking during the aging step due to capillary stresses. The gels were then aged at 60 °C for three days. After 3 days, the aged gels were then unmolded and immersed in a bath composed of 50 vol% isopropanol and 50 vol% water for 4 hours in ambient conditions to remove excess of surfactants and urea. The gels were later washed with isopropanol 5 times within a span of 3 days in room conditions.

After the washing steps, the composite gels were transferred into an autoclave (1 liter) for SC-CO₂ drying and covered with an excess of isopropanol. The drying was performed at 37 °C and 80 bars and the SC-CO₂ dynamic washing step (using a CO₂ mass flow rate of 5 kg/h) was done for 5 hours. A depressurization rate of 4 bar/h at 37 °C was employed to prevent samples from being damaged (e.g. densification or occurrence of cracks).

Composite aerogels were also prepared at a processing temperature of 80 °C (i.e. gelation and ageing steps performed at 80 °C). They were labelled 80CA-0.096, 80CA-0.16, etc.

The whole synthesis steps is provided in



scheme 1.

Scheme 1. Synthesis steps involved in the preparation loop of the present composite aerogels

Characterization of Composite aerogels

The bulk density (ρ_b) was calculated from measurements of the mass and volume of the aerogel. The global linear shrinkage (%) was calculated from the change in diameter between the unaged alcogel and the final dry material (i.e. aerogel).

The mass fraction of PMSQ (W_{PMSQ}) in the composite aerogel was calculated using the equation,

$$W_{PMSQ}(\%) = \left(1 - \frac{m_{\text{fiber}}}{m_{CA}}\right) \times 100$$

Where m_{fiber} is the mass of the fibers in the composite aerogel and m_{CA} is the mass of the final composite aerogel.

The skeletal density of the composites (ρ_s) was measured using a helium pycnometer (AccuPyc 1330 TC, Micromeritics, Norcross, GA, USA) and was found to be $1.13 \text{ g.cm}^{-3} \pm 0.01$.

The (percentage of) porosity was then determined classically as:

$$\varepsilon = (1 - \rho_b / \rho_s) \times 100.$$

Scanning electron microscopy (SEM) images were taken using Zeiss Supra 40 FEG-SEM. Samples were coated with a 7 nm platinum layer with a QUORUM Q150T sputter before imaging. Specific surface area and pore size distribution (PSD) were characterized by N_2 sorption at 77 K by employing ASAP 2020 from Micromeritics. Aerogels were degassed in vacuum for 10 hours at 100 °C before the measurements. The specific surface area was determined by employing the BET equation. The PSD was obtained using Barrett-Joyner-Halenda (BJH) method.

Effective thermal conductivity was measured in a steady-state regime with FOX150 Thermal Conductivity Meter (Laser Comp apparatus) equipped with a custom micro-flow meter developed by CSTB (Hébert Sallée, Grenoble, France). Thermal

conductivity (λ) was calculated from the measurement of heat flow between hot and cold plates maintained at 25 and 15 °C, respectively.

For the mechanical characterization, the composite aerogel tiles ($9 \times 9 \times 1 \text{ cm}^3$) were cut into parallelepiped bars with dimensions, 90 mm in length, 15 mm in width and 10 mm in thickness. The cutting step was performed by Mecatome T180. The 3-points bending tests were performed using a Zwick universal testing machine equipped with a load cell of 100 N. A three-points bending fixture based on ASTM D 790–03 testing procedure was followed. The span (distance between two supports) was 60 mm for the selected sample size ($9 \times 1.5 \times 1 \text{ cm}^3$). These experimental specifications were already reported for low-density aerogels (0.18 g.cm^{-3}) synthesised from tetramethoxysilane (TMOS) [43]. The ratio between the span and the sample thickness is maintained above 5 and hence the modulus does not depend on the sample geometry. The present tests were performed with a loading nose descent rate of 1 mm/min.

The sessile drop (water contact angle) experiments on the composite aerogels were carried out using Drop Shape Analyser DSA-100 (KRUSS- Gmbh). Significant number of 4 μL MilliQ water drops have been gently deposited from the machine itself and later the drop shape was analysed.

Results and Discussion

Properties of PMSQ- kapok composite aerogels processed at 60 °C

It is important to highlight that in order to obtain very low-density aerogels, it is necessary that the sol is highly diluted which will help in decreasing the solid content and increasing the global porosity of the final material (assuming there is no dramatic shrinkage while drying) [44]. When hydrolyzing a trifunctional silane for e.g. MTMS using mild acids (e.g. acetic acid) in a solvent, as the reaction proceeds, more and more hydrophobic species are generated which becomes incompatible with the solvent, which will be most likely polar (alcohols/water). This will lead to phase separation (macroscopic). To avoid these prejudicial phenomena, surfactants were added during our sol-gel process [45].

Within our synthesis frame, gelation times for all the 60 °C processed gels are found to be approximately 5 hours when observed by naked eye. The synthesis of silica-based gels is governed by two mechanisms: 1) hydrolysis of silica-based precursor (viz. MTMS in the present study) and 2) polycondensation of the hydrolyzed species. Within the present sol-gel process the hydrolysis step is governed by the acid catalysis. Indeed, it is well known that

acetic acid (HOAc) is one of the numerous acids able to catalyze hydrolysis of alkoxysilanes. On the other hand, the (poly)condensation process is governed here by the basic catalysis. Indeed, in the presence of water and through thermal activation, urea is known to decompose to ammonium hydroxide (NH_4OH). This base is very classical to catalyze condensation of hydrolyzed alkoxysilanes [1,37]. Due to the specificity of our synthesis route, while increasing the concentration of 5 mM HOAc to the sol-gel system (while keeping constant quantity of MTMS), we also increase urea/MTMS ratio which consequently increases the $\text{NH}_4\text{OH}/\text{MTMS}$ ratio. This theoretically contributes to increase the gelation kinetics and the gelation time remains almost constant for all compositions as a balance between these two mechanisms.

In all probability, it is envisaged that the silanol from the hydrolyzed MTMS and the hydroxyl group present in kapok react to form a crosslinked structure and a possible/probable structure is provided in Fig. 1. The photograph of the samples obtained after SC drying are provided in Fig. 2a. They all appear monolithic and without cracks detectable to the naked eye. It is important to stress that all the sol compositions without the fibers were cracked and hence could not be characterized further. The properties of the composite aerogels processed at 60 °C are summarized in Table 1. It can be clearly seen that the density of the composite aerogels decreases as the HOAc concentration is increased. A maximum density of 0.088 $\text{g}\cdot\text{cm}^{-3}$ was obtained for composite aerogel 60CA-0.16 and a minimum density of 0.061 $\text{g}\cdot\text{cm}^{-3}$ for 60CA-0.096. This is in line with what is generally expected with significant dilution of the silica precursor in reaction media. Besides, even if global shrinkage ratio is experimentally difficult to measure very accurately with simple standard techniques, it seems that it tends to increase slightly with the dilution of the sol. The highest linear shrinkage was observed for the (MTMS)/(HOAc) weight ratio of 0.096. This could be attributed to the lower mechanical resistance of the gels to the different types of stresses appearing all along the synthesis process (i.e. syneresis, drying ...) due to the lower quantities of solid matter (PMSQ phase) in the system. Here, the W_{PMSQ} varies from 62 % (60CA-0.096) to 72% (60CA-0.16). As a conclusion, in our case, the evolution of bulk density with sol-gel formulation permits to state that the predominant effect on this property is concentration of silica precursor in the sol and not shrinkage due to mechanical considerations. The apparent porosity values are also provided in Table 1. All the composite aerogels possessed porosity greater than 90% and a maximum porosity of 95 % was obtained for the less concentrated composite aerogel (60CA-0.096). They could all be considered as hyper-porous materials.

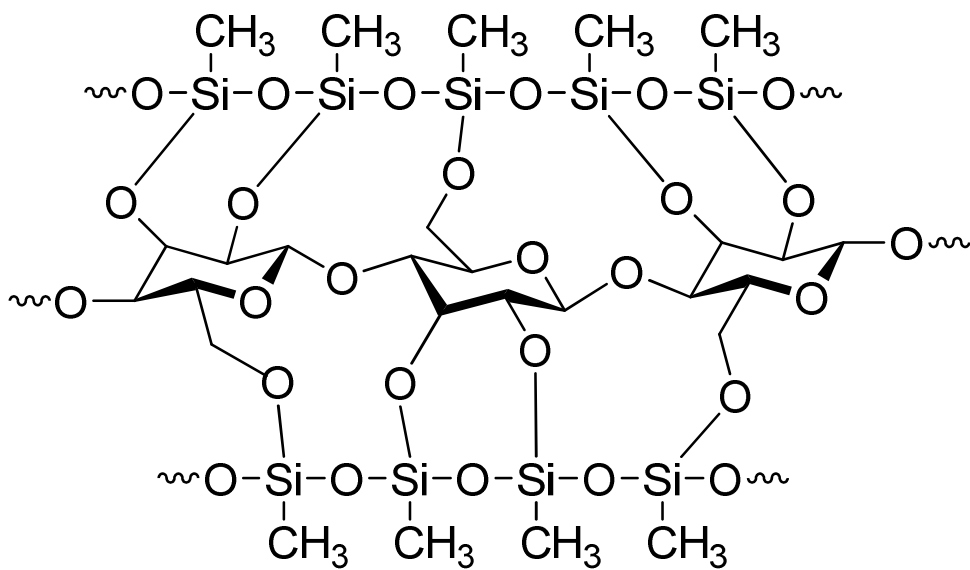


Fig. 1. Possible chemical structure of PMSQ-kapok composite aerogel

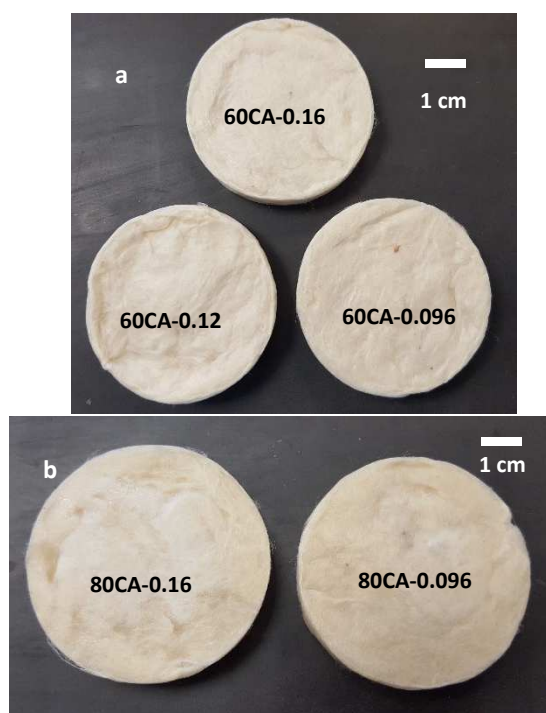


Fig.2. Photograph of composite aerogels processed at 60 °C (a) and 80 °C (b)

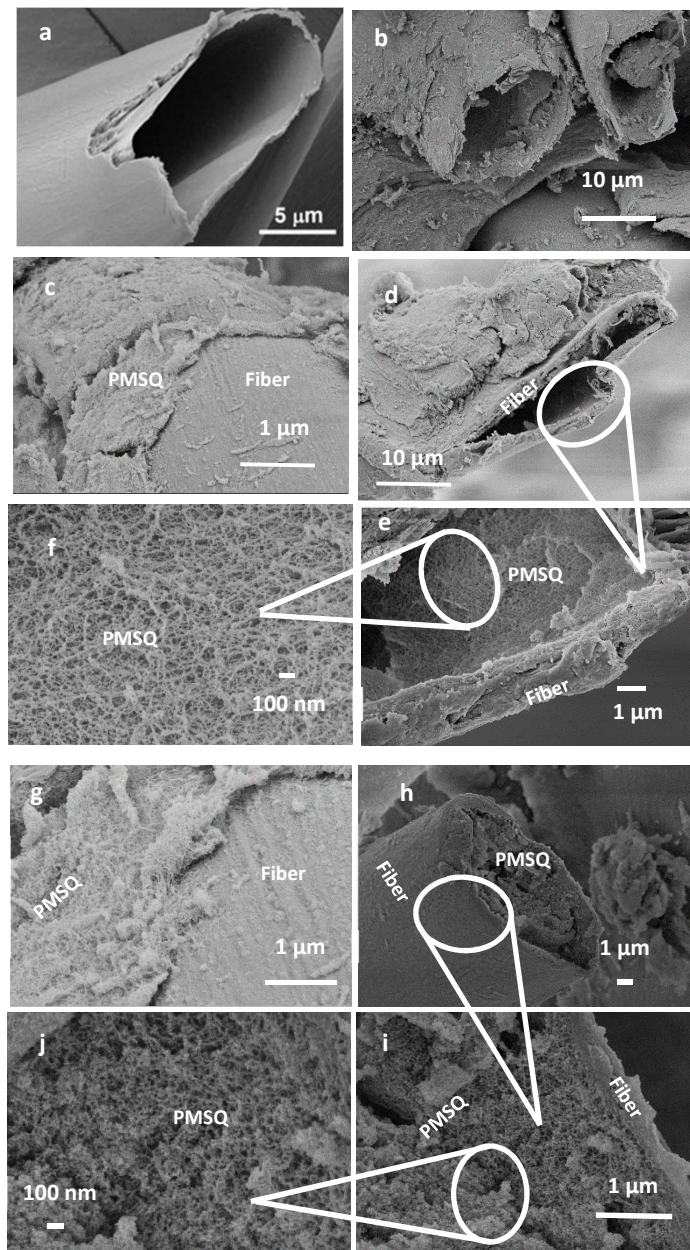


Fig. 3. SEM fractographs of fibers and composites.

a) Kapok fiber (alone),

b) low magnification fractograph demonstrating the overall appearance of the composite material

c) low magnification of composite aerogel 60CA-0.16 showing the PMSQ phase attached to the exterior of the fiber

d) low magnification of PMSQ phase attached/linked to the porous fiber,

e) low magnification of PMSQ aerogel phase inside the fiber,

f) higher magnification of PMSQ aerogel phase

g) low magnification of composite aerogel 80CA-0.16 showing the PMSQ phase linked to the exterior of the fiber

h) low magnification of composite aerogel 80CA-0.16 showing the fiber and the PMSQ phase

i) low magnification fractograph of PMSQ aerogel phase present inside the porous fiber and

j) higher magnification of PMSQ aerogel phase alone.

The SEM fractographs of the Kapok fibers alone and the composite aerogels (60CA-0.16) are provided in Fig. 3. From the fractograph of 60CA-0.16 (Fig. 3b), it can be seen that the PMSQ aerogel is well attached/adhered to the fiber (exterior) as there is no visible gap (macroscopically) between the fiber and the aerogel matrix. The kapok fibers (Fig 3 c,d) still remain partially hollow after the sol-gel transition has occurred. It could also be seen from Fig. 3.d that the PMSQ aerogel seems to be well bonded with the fiber in the interior of the hollow fiber (again with no visible gap (macroscopically) between the fiber and the aerogel). Higher magnification of the PMSQ aerogel (3.e) depicts a structure mostly formed of mesopores with macropores of small characteristic dimensions which matches well with the PSD obtained with BJH model (discussed in the coming paragraph). The SEM fractographs of 60CA-0.096 (Figure S1) is comparable to the one obtained for 60CA-0.16. Based on these SEM fractographs, we can assume that the silanol from the hydrolyzed MTMS and the hydroxyl group present in kapok react to form a crosslinked structure as provided in Fig. 1.

The sorption isotherms of the kapok-based composite aerogels are provided in Fig 4. The isotherms are of Type IV characteristic of mesoporous material. “The PSD graph [inset (Fig. 4)] indicates that the majority of the detected pores are located between 10-40 nm as characterized with BJH technique. It is well-known that BJH model is not very well-suited for silica-based light weight aerogels. Hence there might be necessarily the presence of some undetected larger pores in the silica matrix. However, by looking at the very low level of thermal conductivity (see after), the corresponding porous volume fraction must be very low too.” CTAB has both lipophilic and hydrophilic groups. When its concentration exceeds the first theoretical micelle concentration of 0.89 mmol/L, it will form micelles by self-assembly which results in the decrease of the surface energy of the solution [46]. When the concentration of CTAB is higher than the second theoretical critical micelle concentration of

21 mmol/L, a relatively uniform PSD is reported [47]. In our system, the micelle concentration for MTMS/HOAc = 0.16 is found to be 47 mmol/L while that for MTMS/HOAc = 0.096 is found to be 29 mmol/L which in both cases is higher than the reported second critical micelle concentration of 21 mmol/L. This could explain why we obtain such uniform PSDs whatever our dilution rate. However, in our study, the PSD appears slightly broader and this could probably arise from the partial filling of the hollow tubes by PMSQ aerogel.

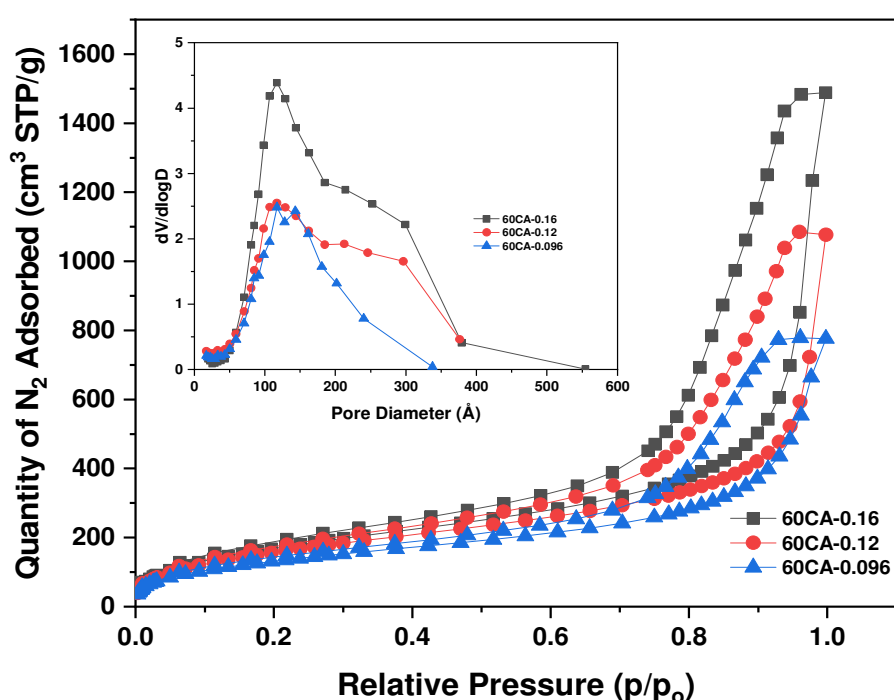


Fig. 4. Sorption isotherms of composite aerogels processed at 60 °C (Inset: PSD of samples synthesized with different dilution levels)

The S_{BET} of the composite aerogels are between 470 and 620 m^2/g and exhibit the same trend with the dilution of the sol (Table 2). First of all, the values are lower when compared with standard silica-based aerogels although the global range is wide. This can simply be explained by the fact that the cellulose fibers do not really contribute to the surface area of the composite as they are neither mesoporous nor rough. Moreover, the fiber mass fraction is also appreciable. It can also be observed that the S_{BET} decreases with dilution because of the reduction in the mass fraction of PMSQ phase in the final material. (Kindly

note that almost the same quantity of composite aerogels was taken for BET analysis). Furthermore, the C parameter (also known as BET constant in the BET equation) provides some indications on the chemical nature of the surface of the materials. It is well known that the C value increases with the polarity. The value of this parameter is around 120 for unmodified standard silica aerogels and with surface modification (i.e. trialkoxysilanes), it drops to 60 [48]. Within this study, the C values for the composite aerogels 60CA-0.16, 60CA-0.12 and 60CA-0.096 are 68, 67 and 77 respectively (Table 1). Hence, we can already infer that these composite aerogels are non-polar or little polar. (Please also refer to the sessile drop results presented just before general conclusion for further elements.)

Finally, the thermal conductivity values for all the composite aerogels synthesized at 60 °C are clearly in the range of thermal superinsulating materials (i.e. values lower than 0.020 W.m⁻¹.K⁻¹ in room conditions). It can be stressed that a thermal conductivity value of 0.0171 W.m⁻¹.K⁻¹ was obtained for the lighter composite aerogels synthesized at 60° C (60CA-0.096 sample which has a bulk density of 0.061 g.cm⁻³). Lower values can be obtained but the corresponding samples present larger bulk densities (e.g. 0.0156 W.m⁻¹.K⁻¹ and 0.088 g.cm⁻³ for 60CA-0.24 sample).

In room conditions, the total thermal conductivity (λ) can be considered as the sum of three decoupled contributions to thermal transfer and can be described as follows: $\lambda = \lambda_s + \lambda_g + \lambda_r$, where λ_s , λ_g and λ_r are the solid, gaseous and radiative contributions, respectively. Our materials are all super-insulating because i) air is confined in a Knudsen regime in the mesoporosity of the PMSQ part of the aerogel (as shown by the N₂ sorption and SEM fractographs, the main pore size (~ 10-40 nm) are lower than mean free path of free air (~ 70 nm), ii) volume fraction of solid matter (considering both silica and kapok) is very low and iii) such materials are nearly opaque to near-infrared radiations at room temperature. However, to produce ultra-light materials with the lowest thermal conductivity as possible, it is necessary to find a delicate balance between solid and gaseous conduction as well as radiation. For instance, decreasing density may permit to reduce solid contribution but decreasing too much may generate too large pores and thus tends to lose benefit of gas confinement in the mesopores as well as a significant increase of radiative transfer. At this point the open question is “Is it possible to improve further the properties of these materials in terms of compromise between effective thermal conductivity and bulk density?”

Properties of PMSQ- Kapok composite aerogels processed at 80 °C¹

At higher temperature, the Brownian motion of the sol particles is higher and the probability of one colloidal silica particle colliding with the other forming a bond is hence higher. It is also reported that the gelation time t_g , (corresponding to sol-gel transition) varies with temperature, T following a simple Arrhenius relationship (2) [49],

$$\frac{1}{t_g} = A e^{\left(\frac{E}{RT}\right)} \quad (2)$$

Therefore, within the frame of this work the gelation time for the 80 °C gel system is thus significantly lower than that of the gels synthesized at 60 °C. It was found to be approximately 3 hours (instead of 5 hours). As we can see from Table 1, there is slightly lesser shrinkage and hence the bulk density of the aerogels are also notably lower for the 80 °C processed gels compared to the 60 °C synthesized ones. It is well known that the aging process facilitates the dissolution and reprecipitation of silica into the gel structure [1]. It is also reported that the degree of reprecipitation of the silica is somehow correlated to the aging temperature [50]. Hence by the aging process at 80 °C, the gel skeleton is mechanically strengthened resulting in lower shrinkage ratios and consequently lower bulk densities.

The photographs of the composite aerogels processed at 80 °C are provided in Fig. 2 b. Their properties are provided in Table 1. A density of 0.071 g.cm⁻³ was obtained for 80CA-0.16 and a density as low as 0.053 g.cm⁻³ was obtained for the 80CA-0.096 composite aerogel. The porosity of these materials is 94-95%. The W_{PMSQ} are 72% and 61% for 80CA-0.16 and 80CA-0.096 samples respectively.

The SEM fractographs of 80CA-0.16 are provided in Fig 3 (f-i). The fractographs are similar to the 60 °C counterparts where it seems the PMSQ aerogel part is well bonded to the fiber. The SEM fractographs of 80CA-0.096 are provided in Figure S3 and it is identical to the one observed for 80CA-0.16.

¹ Composite aerogels without fibers (processed at 80 °C) were also synthesised and the properties (i.e. global shrinkage, bulk density and porosity) are provided in the supplementary information (Table S1). The photographs of some representative samples are provided Figure S2. However, the materials synthesized were very fragile. For instance, the aerogels synthesized with MTMS/HOAC = 0.096 were so fragile that they cracked into pieces while handling them and the ones synthesized with MTMS/HOAC = 0.12 were severely cracked after SC drying. The fragility of these samples was such that it was finally not possible to perform any physical characterizations like thermal conductivity measurement and 3-points bending tests and only the bulk density could be measured.

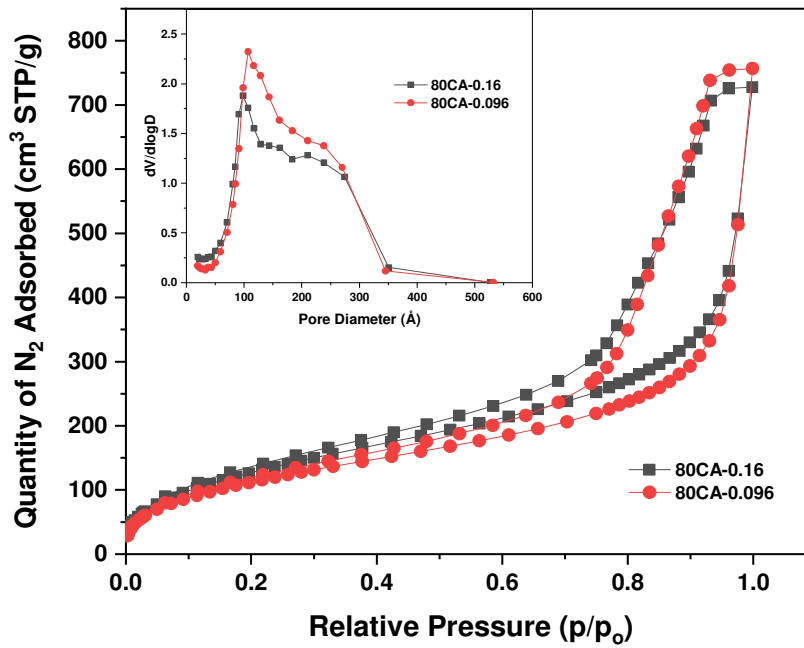


Fig. 5. Sorption isotherms of composite aerogels processed at 80 °C (Inset: PSD of the samples synthesized with different dilution levels)

Again, the sorption isotherms (Fig 5) reveal that the materials are mesoporous due to the Type-IV isotherm. The S_{BET} (Table 1) of 80CA-0.16 and 80CA-0.096 aerogels are 494 and 442 m^2/g respectively. The PSDs provided in the inset (Fig. 5) is similar to the 60 °C counterparts where the majority of pores appears in the 10-40 nm range. The PSD also exhibits some broadness, which may be due the partially filled hollow tubes as evident from the SEM fractographs (Fig. 3).

The thermal conductivity values (Table 1) for the composite aerogels synthesized at 80 °C is also in the range of thermal super insulating materials. A thermal conductivity of $0.0183 \text{ W}\cdot\text{m}^{-1}\cdot\text{K}^{-1}$ was obtained for 80CA-0.096 material which has an extremely low bulk density of $0.053 \text{ g}\cdot\text{cm}^{-3}$. It could also be noticed that the 80CA-0.16 composite aerogel possess also a very low density of $0.071 \text{ g}\cdot\text{cm}^{-3}$ with a lower thermal conductivity of $0.0157 \text{ W}\cdot\text{m}^{-1}\cdot\text{K}^{-1}$ which could also appear as a rather interesting compromise regarding the applicative target of the present study. These results clearly indicate that a very low-density aerogel could also be synthesized at 80 °C by maintaining the super-thermal insulating properties. In fact, the whole results (both 60 and 80 °C) have to be compared with literature. Comparing our results with a rather large panel of what has already been published on this topic (Table 2), we could clearly see that the materials synthesized in this study are very interesting/promising as far as the density and thermal conductivity values are to be considered as a key point in terms of

compromise. The reported results are also compared with some of the commercially available aerogel composite boards/blankets [51-57] (Table 2) and again it is clear that the results presented here are promising.

Mechanical Characterisation

Since the main purpose of our study is to synthesize some composite aerogels with low bulk density together with very low thermal conductivity, mechanical characterization was performed on the samples with the lowest density obtained from the two-processing temperature viz. 60 and 80 °C.

For the mechanical characterization, composite aerogel tiles were synthesized (Fig 6 aI and aII) and cut into sizes of $9 \times 1.5 \times 1 \text{ cm}^3$ lengths as provided in Fig. 6 b. No powder release was observed during engineering and no macroscopic defects due to cutting (e.g. cracks) were observable to the naked eye. Our aerogel composites were studied by 3-points bending tests (Fig. 6c). It is also reported that the flexural modulus E calculated from the 3-points bending provides very accurate results for the trend against the aerogel bulk density. Indeed, the modulus classically calculated from the uniaxial compression experiments (i.e. compressive modulus) is underestimated and their trend against the bulk density is $E \sim (\sigma_{\text{bulk}})^4$ contrary to the flexural modulus $E \sim (\sigma_{\text{bulk}})^3$ [20].

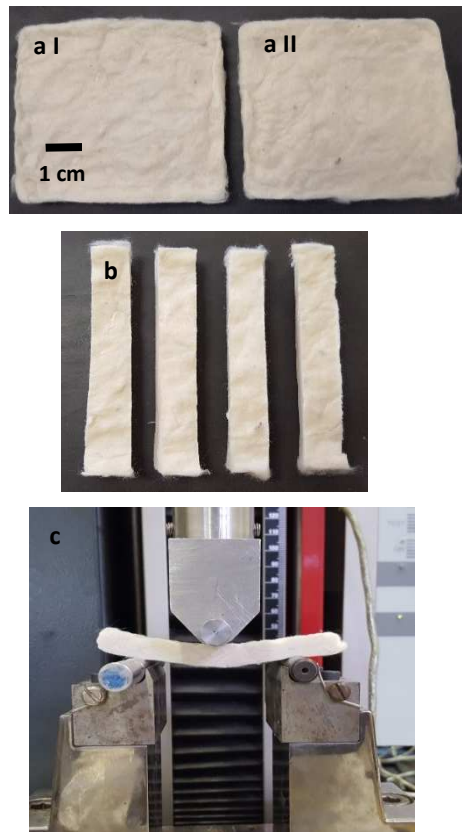


Fig. 6. Photograph of the composite aerogel a) $9 \times 9 \times 1 \text{ cm}^3$ tile: I) 60CA-0.096 and II) 80CA-0.096 samples; b) pieces cut for the mechanical tests, c) view of a typical 3-points bending test.

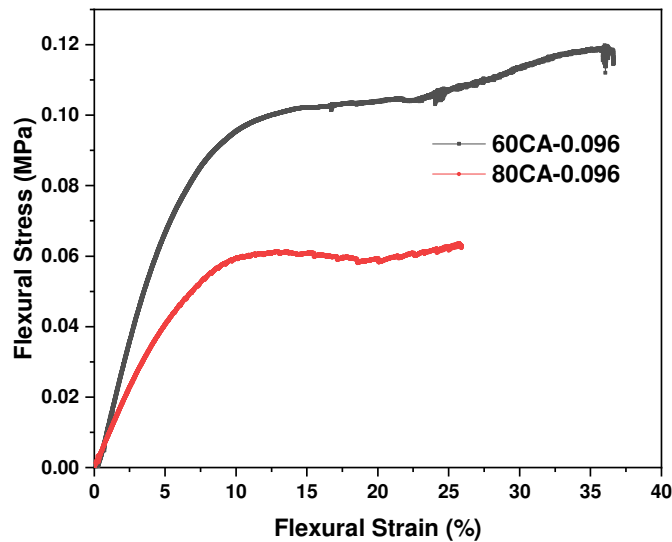


Fig. 7. Stress-strain curves of composite aerogels labelled 60CA-0.096 and 80CA-0.096

The stress-strain graphs of the composite aerogels are plotted in Fig. 7. The formulas for plotting these curves as well as the calculation of the flexural modulus are provided in the supplementary information part. In the present study, the composite aerogel 60CA-0.096

(bulk density of 0.061 g.cm^{-3}) has a flexural strength of $108 \text{ kPa} \pm 21$ (with a flexural modulus of $1.85 \text{ MPa} \pm 0.21$) which is around 2.3 times the flexural strength of classical silica aerogels synthesized with polyethoxydisiloxanes (e.g. 46 kPa for a bulk density of 0.103 g.cm^{-3} [20]). The composite aerogel processed at $80 \text{ }^\circ\text{C}$ (viz. 80CA-0.096) possesses a flexural strength of $62.5 \text{ kPa} \pm 0.7$ and the flexural modulus is calculated to be $1.21 \text{ MPa} \pm 0.06$. However, the density of the composite aerogel is $0.053 \pm 0.002 \text{ g.cm}^{-3}$ which is around half of that of classical PEDS-Px aerogel reported (46 kPa for a bulk density of 0.103 g.cm^{-3}).

To go further, comparison with reinforced silica aerogels described in literature is necessary. To do so, it is very important to compare the mechanical properties obtained with the same characterization method (here, 3-point bending by which flexural strength is measured). The reported results on silica-based composite aerogels characterised by 3-point bending are very few (Table 3). A maximum flexural strength of $150\text{-}200 \text{ kPa}$ with a flexural modulus between $5\text{-}10 \text{ MPa}$ was reported for the silica aerogels synthesized with electrospun polyurethane nanofibers [14]. The maximum density reported here was 0.172 g.cm^{-3} with a low thermal conductivity of $0.013 \text{ W.m}^{-1}.\text{K}^{-1}$. The reinforcement performed with aramid fibers provided a composite aerogel with a maximum bending modulus of 140 kPa and a bending modulus of 1.4 MPa [16]. This composite possessed a density of 0.142 g.cm^{-3} with a thermal conductivity of $0.0236 \text{ W.m}^{-1}.\text{K}^{-1}$. Zhou et al. reported a glass fiber reinforced silica aerogel where a flexural modulus of 1.25 MPa for a composite aerogel possessing a density of 0.175 g.cm^{-3} with a thermal conductivity of $0.0248 \text{ W.m}^{-1}.\text{K}^{-1}$ [58]. A modulus of elasticity of 77.35 and 62.8 MPa was reported for silica aerogels with Au and Ag dispersed nanoparticles possessing a density of 0.56 and 0.58 g.cm^{-3} respectively [29]. A basalt fiber reinforced aerogel resulted in a composite with a maximum bending stress of 33 kPa [59]. A maximum flexural strength of 184 kPa was reported for Lyocell reinforced composite aerogel. The density of the composite was 0.125 g.cm^{-3} with a thermal conductivity of $0.0175 \text{ W.m}^{-1}.\text{K}^{-1}$ [20]. The flexural strength of classical silica aerogels synthesized with polyethoxydisiloxanes (PEDS-Px) is 46 kPa possessing a bulk density of 0.103 g.cm^{-3} [20]. For all these reinforced samples, when thermal conductivity is acceptable for super-insulating applications, bulk density appears clearly too high to target special sphere.

Thinner composite aerogel sheets

To tackle different kind of applications, thinner composite aerogels were prepared (approx. 2 mm-thick) and the corresponding sheets could be rolled without dust release (Fig. 8) [supplementary information for the aerogel rolling video]. This could be very advantageous and could be used to insulate for instance the edges, corners, etc.



Fig. 8. Photographs of a thin kapok-based composite aerogel sheet (sample 80CA-0.096 with dimensions close to 9 cm x 9 cm x 0.2 cm, unfolded and rolled, respectively).

Contact angle measurements of composite aerogels

The contact angle measurement (sessile drop) performed on the composite aerogel is illustrated in Fig. 9. The 60CA-0.096 samples provided a contact angle of $140^\circ \pm 5$. This result confirms that the present composite aerogels are hydrophobic. It is also reported in the literature that the aerogels derived from trifunctional silane precursor leads to a hydrophobic aerogel due to the presence of the functional methyl groups [60]. Without any specific silylation step these composite materials are intrinsically hydrophobic (viz. due to the methyl groups present in the precursor and also as a result of the crosslinked aerogel structure depicted in Fig 1). Addition of cellulosic reinforcement charge (intrinsically hydrophilic) does not degrade this very important property regarding thermal insulation application. It can be noticed that this result endorses the C parameter values obtained from BET surface area measurements presented and commented before.



Fig. 9. Water droplets (4 μl) on the surface of a PMSQ-Kapok composite aerogel

Conclusions

Composite aerogels synthesized with MTMS as silica precursor and kapok fibers as reinforcing additives exhibit very promising results in terms of a compromise between bulk density and effective thermal conductivity. Indeed, it has been shown in this work that bulk density could reach very low levels without degrading extreme quality of thermal conductivity presented by standard silica aerogels. It has been demonstrated that increasing temperature of the sol-gel synthesis process and using hollow fibers permits to tune finely the density – thermal conductivity couple. A density of 0.053 gcm^{-3} with a thermal conductivity of $0.018 \text{ W.m}^{-1}.\text{K}^{-1}$ was obtained. Besides, the samples are intrinsically hydrophobic and from a mechanical point of view they can be considered as reinforced (maximum flexural stress of 108 kPa) compared to classical silica aerogels synthesized from polyethoxydisiloxane. A comparison with literature stressed that no equivalent materials have been described until now.

Finally, it has also be shown that decreasing their thickness, they become rollable like standard silica-based blankets. As they do not powder, these new aerogels can thus be considered as really promising candidates for uses where the embedded mass is crucial (for example, space applications).

CRedit authorship

Parakkulam Ramaswamy Aravind: Methodology, Investigation, Writing- Original Draft, Writing- Review and editing.

Arnaud Rigacci: Conceptualisation, Funding acquisition, Supervision, Writing- Review and Editing.

Declaration of competing interest

The authors declared no conflicts of interest to this work.

Acknowledgements

The authors would like to acknowledge The Centre National d'Etudes Spatiales (CNES, France) for funding this project. The authors warmly thank Prof. Dr. Gian Domenico Soraru, University of Trento for the helium pycnometry characterisations. The authors thank Pierre Ilbizian (PERSEE - MINES ParisTech) for SC- CO₂ drying, Suzanne Jacomet for SEM characterization, Cyrille Collin for engineering the aerogels for mechanical testing and Gilbert Fiorucci for the mechanical testing, all three from CEMEF - MINES ParisTech. The authors are very grateful to Dr. Gediminas Markevicius for the fruitful discussions.

References

- [1] C.J. Brinker, G.W. Scherer (1989) *Sol-Gel Science: The Physics and Chemistry of Sol-Gel Processing* Academic Press, New York.
- [2] M.M. Koebel, A. Rigacci, P. Achard (2011) *Aerogels for Superinsulation: A Synoptic View*. In: Aegerter MA, Leventis N, Koebel, MM (eds) *Aerogels Handbook*, Aerogels handbook. Springer, New York, pp 607-633
- [3] S.S. Kistler Coherent Expanded Aerogels and Jellies, *Nature* 127 (1931) 741.
- [4] G. Zhang, A. Dass, A-M.M. Rawashdeh, J. Thomas, J.A. Council, C. Sotiriou-Leventis, E.F. Fabrizio, F. Ilhan, P. Vassilaras, D. Scheiman, L. McCorkle, A. Palczar, J.C. Johnston, M.A.B. Meador, N. Leventis, Isocyanate-crosslinked silica aerogel monoliths: preparation and characterization. *J Non-Cryst Solids* 350 (2004) 152–64.
- [5] A. Katti, N. Shimpi, S. Roy, H. Lu, E.F. Fabrizio, A. Dass, L.A. Capadona, N. Leventis, Chemical, Physical, and Mechanical Characterization of Isocyanate Cross-linked Amine-Modified Silica Aerogels. *Chem Mater* 18(2) (2006) 285–296
- [6] N. Leventis, Three-Dimensional Core-Shell Superstructures: Mechanically Strong Aerogels. *Acc Chem Res* 40(9) (2007) 874-84
- [7] M.A.B. Meador, A.S. Weber, A. Hindi, M. Naumenko, L. McCorkle, D. Quade, S.L. Vivod, G.L. Gould, S. White, Deshpande K Structure-property relationships in porous 3D nanostructures: epoxy-crosslinked silica aerogels produced using ethanol as the solvent, *ACS Appl Mater Interfaces* 1(4) (2009) 894–906.

- [8] B.N. Nguyen, M.A.B. Meador, A. Medoro, V. Arendt, J. Randall, L. McCorkle, B. Shonkwiler, Elastic Behavior of Methyltrimethoxysilane Based Aerogels Reinforced with Tri-Isocyanate, *ACS Appl Mater Interfaces* 2(5) (2010) 1430–1443
- [9] H. Maleki, L. Durães, A. Portugal, An overview on silica aerogels synthesis and different mechanical reinforcing strategies. *J Non-Cryst Solids* 385 (2014) 55–74.
- [10] T. Linhares, M.T. Pessoa de Amorim, L. Durães, Silica aerogel composites with embedded fibres: a review on their preparation, properties and applications, *J Mater Chem A* 7 (2019) 22768-22802.
- [11] J.K. Lee (2007) US patent US20070259979A1
- [12] Z. Zhang, J. Shen, X. Ni, G. Wu, B. Zhou, M. Yang, X. Gu, M. Qian, Y. Wu, Hydrophobic Silica Aerogels Strengthened with Nonwoven Fibers. *J. Macromol. Sci. Part A* 43 (2006) 1663–1670.
- [13] D.H. Blount (1990) US Patent US4954327A
- [14] L. Li, B. Yalcin, B.N. Nguyen, M.A.B. Meador, M. Cakmak, Flexible Nanofiber-Reinforced Aerogel (Xerogel) Synthesis, Manufacture, and Characterization. *ACS Appl Mater Interfaces* 1(11) (2009) 2491–2501.
- [15] H. Wu, Y. Chen, Q. Chen, Y. Ding, X. Zhou, H. Gao, Synthesis of Flexible Aerogel Composites Reinforced with Electrospun Nanofibers and Microparticles for Thermal Insulation. *J Nanomater* 2013 (2013) 1–8.
- [16] Z. Li, X. Cheng, S. He, X. Shi, L. Gong, H. Zhang, Aramid fibers reinforced silica aerogel composites with low thermal conductivity and improved mechanical performance, *Composites, Part A* 84 (2016) 316- 325.
- [17] J.C.H. Wong, H. Kaymak, P. Tingaut, S. Brunner, M.M. Koebel, Mechanical and thermal properties of nanofibrillated cellulose reinforced silica aerogel composites. *Microporous Mesoporous Mater.* 217 (2015) 150–158.
- [18] S. Zhao, W.J. Malfait, A. Demilecamps, Y. Zhang, S. Brunner, L. Huber, P. Tingaut, A. Rigacci, T. Budtova and M. M. Koebel Strong, Thermally Superinsulating Biopolymer–Silica Aerogel Hybrids by Cogelation of Silicic Acid with Pectin, *Angew Chem Int Ed* 54 (2015) 14282–14286.

- [19] G. Markevicius, R. Ladj, P. Niemeyer, T. Budtova, A. Rigacci, Ambient-dried thermal superinsulating monolithic silica-based aerogels with short cellulosic fibers, *J Mater Sci* 52(4) (2017) 2210–21.
- [20] J. Jaxel, G. Markevicius, A. Rigacci, T. Budtova, Thermal superinsulating silica aerogels reinforced with short man-made cellulose fibers, *Composites: Part A* 103 (2017) 113-121.
- [21] Z. Deng, J. Wang, A. Wu, J. Shen, B. Zhou, High strength SiO₂ aerogel insulation, *J. Non-Cryst Solids* 225 (1998) 101–104.
- [22] Y. Liao, H. Wu, Y. Ding, S. Yin, M. Wang, A. Cao, Engineering thermal and mechanical properties of flexible fiber-reinforced aerogel composites, *J Sol- Gel Sci Technol* 63 (2012) 445–456.
- [23] X. Li, Q. Wang, H. Li, H. Ji, X. Sun, J. He, Effect of sepiolite fiber on the structure and properties of the sepiolite/silica aerogel composite, *J. Sol-Gel Sci. Technol* 67 (2013) 646–653.
- [24] Z. Shao, X. He, Z. Niu, T. Huang, X. Cheng, Y. Zhang, Ambient pressure dried shape-controllable sodium silicate based composite silica aerogel monoliths. *Mater Chem Phys* 162 (2015) 346–353.
- [25] J. Li, Y. Lei, D. Xu, F. Liu, J. Li, A. Sun, J. Guo, G. Xu, Improved mechanical and thermal insulation properties of monolithic attapulgite nanofiber/silica aerogel composites dried at ambient pressure. *J Sol-Gel Sci. Technol.* 82 (2017) 702–711.
- [26] X. Hou, R. Zhang, D. Fang, An ultralight silica-modified ZrO₂–SiO₂ aerogel composite with ultra-low thermal conductivity and enhanced mechanical strength, *Scr. Mater.* 143 (2018) 113–116.
- [27] X. Hou, R. Zhang, D. Fang, Novel whisker-reinforced Al₂O₃–SiO₂ aerogel composites with ultra-low thermal conductivity. *Ceram. Int.* 43 (2017) 9547–9551.
- [28] A. Demilecamps, G. Reichenauer, A. Rigacci, T. Budtova, Cellulose–silica aerogels, *Cellulose* 21 (2014) 2625–2636.
- [29] M.F. Bertino, J.F. Hund, G. Zhang, C. Sotiriou-Leventis, A.T. Tokuhira, N. Leventis, Room Temperature Synthesis of Noble Metal Clusters in the Mesopores of Mechanically Strong Silica-Polymer Aerogel Composites, *J. Sol-Gel Sci. Technol.* 30 (2004) 43–48.

- [30] L. Franzel, C. Wingfield, M.F. Bertino, S. Mahadik-Khanolkar, N. Leventis, Regioselective cross-linking of silica aerogels with magnesium silicate ceramics, *J Mater Chem A* 1 (2013) 6021–6029.
- [31] S. Motahari, H. Javadi, A. Motahari, Silica-Aerogel Cotton Composites as Sound Absorber. *J. Mater Civ Eng* 27 (2015) 1–6
- [32] E. Rezaei, J. Moghaddas, Thermal conductivities of silica aerogel composite insulating material. *Adv Mater Lett* 7 (2016) 296–301.
- [33] J. Cai, S. Liu, J. Feng, S. Kimura, M. Wada, S. Kuga, L. Zhang, Cellulose–Silica Nanocomposite Aerogels by In Situ Formation of Silica in Cellulose Gel. *Angew. Chem. Int. Ed.* 51 (2012) 2076–2079.
- [34] S. Zhao, Z. Zhang, G. Sèbe, R. Wu, R.V.R. Virtudazo, P. Tingaut, M.M. Koebel, Multiscale assembly of superinsulating silica aerogels within silylated nanocellulosic scaffolds: Improved mechanical properties promoted by nanoscale chemical compatibilization, *Adv. Func. Mater.* 25(15) (2015) 2326-2334.
- [35] J. Zhang, Y. Cheng, M. Tebyetekerwa, S. Meng, M. Zhu, Y. Lu, Stiff–Soft” Binary Synergistic Aerogels with Superflexibility and High Thermal Insulation Performance. *Adv Funct Mater* 29(15) (2019) 1806407-1806417.
- [36] S. Jiang, M. Zhang, M. Li, L. Liu, L. Liu, J. Yu, Cellulose nanofibril (CNF) based aerogels prepared by a facile process and the investigation of thermal insulation performance. *Cellulose* 27 (2020) 6217-6233.
- [37] K Kanamori, M Aizawa, K Nakanishi, T Hanada, New Transparent Methylsilsesquioxane Aerogels and Xerogels with Improved Mechanical Properties. *Adv. Mater.* 19 (2007) 1589-1593.
- [38] G Hayase, K Kanamori, A Maeno, H Kaji, K Nakanishi, Dynamic spring-back behavior in evaporative drying of polymethylsilsesquioxane monolithic gels for low-density transparent thermal superinsulators. *J Non-Cryst Solids* 434 (2016) 115–119.
- [39] Y Li, A Du, J Shen, Z Zhang, G Wu, B Zhou, Temperature dependence of dynamic mechanical behaviors in low density MTMS-derived silica aerogel. *J Porous Mater* 25 (2018) 1229-1235.

- [40] T Li, A Du, T Zhang, W Ding, M Liu, J Shen, Z Zhang, B Zhou, Efficient preparation of crack-free, low-density and transparent polymethylsilsesquioxane aerogels via ambient pressure drying and surface modification RSC Advances, 8 (2018) 17967-17975.
- [41] Y. Zheng, A. Wang, Kapok Fiber: Applications. In: Khalid Rehman Hakeem, Mohammad Jawaid, Umer Rashid (eds) Biomass and Bioenergy Applications, Springer, (2014) pp 251-266
- [42] Y. Zheng, J. Wang, Y. Zhu, A. Wang, Research and application of kapok fiber as an absorbing material: A mini review, J. Enviro Sci. 27 (2015) 21–32.
- [43] A.H. Alaoui, T. Woignier, G.W. Scherer, J. Phalippou, Comparison between flexural and uniaxial compression tests to measure the elastic modulus of silica aerogel. J. Non-Cryst. Solids 354(40–41) (2008) 4556–4561.
- [44] G. Hayase, K. Kanamori, A. Maeno, H. Kaji, K. Nakanishi, Dynamic spring-back behavior in evaporative drying of polymethylsilsesquioxane monolithic gels for low-density transparent thermal superinsulators. J. Non-Cryst. Solids 434 (2016) 115-119.
- [45] G. Hayase, K. Kanamori, K. Nakanishi, Structure and properties of polymethylsilsesquioxane aerogels synthesized with surfactant n-hexadecyltrimethylammonium chloride, Micro. Meso. Mater. 158: (2012) 247-252.
- [46] V. Patel, N. Dharaiya, D. Ray, V.K. Aswal, P. Bahadur, pH-controlled size/shape in CTAB micelles with solubilized polar additives: A viscometry, scattering and spectral evaluation. Colloids Surf A: Physicochem. Eng. Asp. 455 (2014) 67-75.
- [47] X. Li, Z. Yang, K. Li, S. Zhao, Z. Fei, Z. Zhang, A flexible silica aerogel with good thermal and acoustic insulation prepared via water solvent system. J Sol-Gel Sci and Technol 92 (2019) 652-61.
- [48] N. Huesing, U. Schubert, K. Misof, P. Fratzl, Formation and Structure of Porous Gel Networks from Si (OMe)₄ in the Presence of A(CH₂)_nSi(OR)₃ (A = Functional Group). Chem. Mater. 10(10) (1998) 3024-3032.
- [49] M.W. Colby, A. Osaka, J.D. Mackenzie, Effects of temperature on formation of silica gel. J. Non-Cryst. Solids 82(1-3) (1986) 37.
- [50] R.K. Iler The Chemistry of Silica Wiley, (1979) New York

- [51] <https://www.aerogel.com/products-and-solutions/product-documents/>
- [52] <https://www.cabotcorp.com/solutions/products-plus/aerogel/blanket>
- [53] https://local.armacell.com/fileadmin/cms/corporate/en/onepager_armagel/Downloads/technical-datasheet/ArmaGelHT_Technical_Datasheet_English.pdf
- [54] <https://enersens.eu/skogar/>
- [55] <https://nanoaerogel.en.made-in-china.com/product/sBgmqxHunvhK/China-10mm-Aerogel-Blanket-Fma450-for-Wall-Insulation-ASTM-Reports-Available.html>
- [56] <https://nanoaerogel.en.made-in-china.com/product/bBmJypMYOgVE/China-Super-Thermal-Insulation-Silica-Aerogel.html>
- [57] <https://www.activeaerogels.com/flexible-panel/>
- [58] T. Zhou, X. Cheng, Y. Pan, C. Li, L. Gong, H. Zhang, Mechanical performance and thermal stability of glass fiber reinforced silica aerogel composites based on co-precursor method by freeze drying, *Appl. Surface Sci.*, 437 (2018) 321-328.
- [59] T. Becker, D. Pico, J. Lipin, T. Lehmann, A. Luking, M. Hitz, T. Gries, Novel Insulation Material Based on Basalt Fibres and Silica Aerogels, *Chemical Engineering Transactions*, 73 (2019) 49-54.
- [60] P. R. Aravind and G. D. Soraru, *J. Porous Mater.* 18 (2011) 159–165.

Table 1. Synthesis parameters and main properties of PMSQ-Kapok composite aerogels synthesized at 60 and 80 °C

Sample	(MTMS) / (HOAc) ¹	Linear shrinkage (%)	ρ (g/cm ³)	ε (%)	λ W.m ⁻¹ .K ⁻¹ ± 0.0005	S _{BET} (m ² /g)	C Parameter	W _{PMSQ} (%)
60 °C treated aerogels								
60CA-0.16	0.16	5.1 % ± 0.5	0.088 ± 0.003	92.2 ± 0.1	0.0156	618 ± 31	68	71.9% ± 0.1
60CA-0.12	0.12	5.4 % ± 0.2	0.075 ± 0.004	93.4 ± 0.3	0.0162	575 ± 24	67	67.1 % ± 0.3
60CA-0.096	0.096	6 % ± 0.7	0.061 ± 0.002	94.5 ± 0.1	0.0171	478 ± 17	77	61.8 % ± 0.1
80 °C treated aerogels								
80CA-0.16	0.16	3.8 % ± 0.1	0.071 ± 0.004	94.0 ± 0.1	0.0157	494 ± 13	64	71.8 % ± 0.5
80CA-0.096	0.096	4.3 % ± 0.1	0.053 ± 0.002	95.3 ± 0.1	0.0183	442 ± 12	70	61.0 % ± 0.2

¹Weight Ratio

* MTMS/HOAC = 0.12 (80 °C)

Table 2. Properties of some composite aerogels reported in the literature

Reinforcement method (e.g. fillers, ...)	ρ (g.cm ⁻³)	λ (W.m ⁻¹ .K ⁻¹) (T)*	Reference
Organic fiber Reinforcement			
Electrospun polyurethane fibers	0.172	0.0130 (20 °C)	Li L et al. [14]
Electrospun Polyvinylidene fibers	0.202	0.0270	Wu H et al. [15]
Aramid fibers (KEVLAR®)	0.142	0.0236 (25 °C)	Li Z et al. [16]
Nanofibrillated cellulose water suspension	0.131	0.0142	Wong JCH et al. [17]
Pectin nanofibers	0.13	0.0142	Zhao S et al. [18]
Lyocell fibers (Tencel®)	0.105	0.0170	Markevicius G et al. [19]
Lyocell fibers (Tencel®)	0.125	0.0175	Jaxel J et al. [20]
Impregnation of coagulated cellulose with PEDS solution	0.155	0.0280	Demilecamps A et al. [28]
Fibrillar cellulose hydrogel- silica composite	0.14	0.0250	Cai J et al. [33]
Silica network synthesized inside silylated nanofibrillated network	0.13	0.0138	Zhao S et al. [34]
Bacterial cellulose aerogel in PMSQ domains	0.09	0.0150	Zhang J et al. [35]

* As there was little difference in the porosity and λ values of samples synthesized at 60°C with MTMS/HOAC ratios of 0.16 and 0.12, it was decided to omit the MTMS/HOAC ratio of 0.12 for the samples processed at 80 °C.

Cellulose nanofibers/methyltrimethoxysilane/fumed silica	0.02	0.0270	Jiang S et al. [36]
Inorganic fiber reinforcement			
Ceramic fibers	0.185	0.0220 (100 °C)	Deng Z et al. [21]
Glass fibers	0.163	0.0240 (25 °C)	Liao Y et al. [22]
Sepiolite fibers	0.210	0.0250 (50 °C)	Li X et al. [23]
Silica fibers	0.104	0.0220	Shao Z et al. [24]
Attapulgitic fibers	0.173	0.0198	Li J et al. [25]
Zirconia fibers	0.290	0.0262 (25 °C)	Hou X et al. [26]
Aluminium borate whiskers	0.350	0.0400	Hou X et al. [27]
Commercially available composite aerogel sheets/blankets			
Pyrogel HPS (ASPEN)**	0.2	0.022 (25 °C)	[51]
Cryogel HPS (ASPEN)	0.16	0.017	[51]
Spaceloft (Cabot)	0.16	0.015	[52]
Armagel DT (Jios Aerogel)	0.16-0.24	0.021 (24 °C)	[53]
Skogar (Enersens)	0.175	0.011-0.013	[54]
Aerogel blanket Fma 450 (Nano Tech co. Ltd)	0.18-0.21	0.018 (25 °C)	[55]
Superthermal insulation silica aerogel (Nano Tech co. Ltd)	0.2	0.018 (25 °C)	[56]
Siliflex (Active aerogels)	0.105	24.9	[57]
Current study			

<i>60CA-0.096 samples</i>	<i>0.061</i>	<i>0.0171</i>	
<i>80CA-0.096 samples</i>	<i>0.053</i>	<i>0.0183</i>	

** Thermal conductivity measurement temperature in brackets. When not notified by the authors means measured at “room temperature”*

***Product name and company name in brackets*

Table 3. Mechanical properties of the composite aerogels reported in the literature in comparison with the present study

Reinforcement	Flexural Strength (kPa)	Flexural modulus (MPa)	Density (gcm⁻³) (Reinforced)	Thermal conductivity (W.m⁻¹.K⁻¹) (T)*	Reference
Electrospun polyurethane fiber	150-200	5-10	0.079-0.172	0.013-0.051 (20 °C)	Li L et al. [14]
Aramid fibers (KEVLAR®)	140 (Bending strength)	1.4 (Bending modulus)	0.142	0.0235 (25 °C)	Li Z et al. [16]
Nanoparticles	-	62.8-77.35(modulus of elasticity)	0.56-0.58	-	Bertino MF et al. [29]
Glass Fiber	-	1.25	0.175	0.025	Zhou T et al. [58]
Basalt fibers	33	-	-	-	Becker T et al. [59]
Lyocell fibers (Tencel®)	19-184.4	0.32-6.86	0.108-0.125	0.0158-0.0181	Jaxel J et al. [20]
Neat silica aerogel	46.3	1.9	0.103	0.0142	Jaxel J et al. [20]
<i>Current study</i>					
<i>60CA-0.096</i>	<i>108 kPa ± 21</i>	<i>1.85±0.21 MPa</i>	<i>0.061</i>	<i>0.0171</i>	
<i>80CA-0.096</i>	<i>62.5kPa ± 0.7</i>	<i>1.21 MPa ± 0.06</i>	<i>0.053</i>	<i>0.0183</i>	

** Thermal conductivity measurement temperature in brackets. When not notified by the authors means measured at “room temperature”*

Superinsulating composite aerogels from polymethylsilsesquioxane and kapok fibers

Aravind Parakkulam Ramaswamy, Arnaud Rigacci

